

# **Smart Manufacturing and Material Processing** (SMMP)

DOI: http://doi.org/10.26480/smmp.01.2023.15.18





#### RESEARCH ARTICLE

## PREPARATION AND PORE STRUCTURE OF NI-CR-MO-CU POROUS MATERIALS WITH SECOND ORDER GRADIENT PORE SIZE

Gan Xiao<sup>a</sup>, Siwei Tan<sup>a</sup>, Baogang Wang<sup>a</sup>, Junsheng Yang<sup>a</sup>, Wenkai Jiang<sup>a\*</sup>, A. Ngatin<sup>b</sup>

- a School of Mechanical Engineering, Wuhan Polytechnic University, Wuhan, Hubei, China
- <sup>b</sup> Department of Chemical Engineering, Politeknik Negeri Bandung, Bandung, Indonesia
- \*Corresponding Author Email: jiangwenk@whpu.edu.cn

This is an open access article distributed under the Creative Commons Attribution License CC BY 4.0, which permits unrestricted use, distribution, and reproduction in any medium, provided the original work is properly cited.

#### **ARTICLE DETAILS**

#### Article History:

Received 20 January 2024 Revised 18 February 2024 Accepted 11 March 2024 Available online 13 March 2024

#### **ABSTRACT**

The activation reaction sintering method was utilized to produce a Ni-Cr-Mo-Cu porous matrix using Ni, Cr, Mo, and Cu powders as raw materials. The vacuum sintering process was then used to create a Ni-Cr-Mo-Cu porous material with larger particle sizes painted on the surface of the matrix. The resulting material with first order gradient pore size was used as the matrix, which was then painted with fine particle size Ni, Cr, Mo, and Cu to obtain second order gradient pore size porous material. The phase, morphology, element distribution, and pore structure parameters of these materials were analyzed, and it was found that they have a uniform element distribution and a complete pore structure. The first order porous material had a maximum pore size of 10.4 µm and a permeability of 83.7 m<sup>3</sup>·m<sup>-2</sup>·h<sup>-1</sup>·KPa<sup>-1</sup>, while the second border porous material had a maximum pore size of 7.2  $\mu m$  and a permeability of 78.9  $m^3 \cdot m^{-2} \cdot h^{-1} \cdot KPa^{-1}$ . Compared to the first order gradient pore size, the second order gradient pore size of the porous material decreased by 30.7%, but the permeability remained basically unchanged, indicating that the permeability of the second order gradient pore size porous material had significantly improved. In summary, using the activation reaction sintering method, a Ni-Cr-Mo-Cu porous material was fabricated, which was later used to construct a gradient pore size porous material with improved permeability. The resulting material had a uniform element distribution and a complete pore structure, making it highly promising for potential applications in filtration, catalysis, and sensing fields.

## **KEYWORDS**

Ni-Cr-Mo-Cu, gradient film, porous material, pore structure, permeability, filtration

## 1. Introduction

Porous metal is a lightweight and porous material that has been developed through advancements in material preparation and processing technology. This innovative material combines the advantages of both structural and functional materials, exhibiting exceptional qualities such as high thermal conductivity, resistance to extreme temperatures, porosity, a large surface area, and the ability to customize its porous structure (Lakhdar et al., 2021; Wang et al., 2013; Xu et al., 2016; Li et al., 2020). In China's economy, the iron and steel industry play a significant role as a foundation sector that integrates capital, technology, and energy. However, this industry also contributes significantly to air pollution, which poses risks to human health and the environment. The use of fossil fuels and other harmful materials has led to increased levels of pollutants such as carbon monoxide, nitrogen oxides, and sulfur oxide (Wu et al., 2023; Vaisnav and Murugesan, 2022). To address this issue, metal foam materials have gained increasing importance in filtration applications. They are widely used in both daily life and industrial settings. These materials possess unique properties and characteristics that make them effective in reducing air pollutants. Therefore, they offer a promising solution to environmental concerns and can greatly improve the overall quality of life (Zhu et al., 2022; Adeniran et al., 2017; Hashe and Jen, 2020).

By utilizing porous materials made from Ni-Cr-Mo-Cu alloys, it is possible to improve air filtration efficiency and effectively remove harmful substances. The porous structure of these materials allows for pollutants

to be trapped and retained, preventing their release into the atmosphere. Additionally, their high thermal conductivity allows for efficient heat transfer, contributing to their excellent filtration performance. Furthermore, the ability to customize the pore structure of these materials opens numerous possibilities for tailoring their filtration capabilities to specific requirements (Umamungu et al., 2022). Moreover, they have the potential to achieve precise control over particle size and distribution, making them ideal for use in air and water filtration systems, as well as in separating various substances.

In recent times, researchers have been exploring various techniques for creating porous materials with improved filtration and separation properties. One approach is to utilize advanced manufacturing techniques such as 3D printing and electrodeposition (Ameta et al., 2022). These methods allow for accurate control over the design and fabrication of the porous structures, enabling the creation of materials with customized properties. Another method involves the integration of functional additives into the porous metal matrix. These additives enhance the filtering efficiency by promoting specific interactions with the target substances. For instance, the addition of nanoparticles with catalytic properties can effectively eliminate harmful pollutants by facilitating chemical reactions. To meet the demand for efficient filtration and separation materials, there is a need for innovative designs in porous metal materials. The development of gradient porous materials with superior filtering quality holds great promise (Li et al., 2015).

Quick Response Code Access this article online



Website:

Website: www.topicsonchemeng.org.my

DOI:

10.26480/smmp.01.2023.15.18

Ti-Al gradient porous materials were effectively created by He et al. utilizing high purity Al powder as the matrix and mixed Ti and Al powder as the gradient layer (He et al., 2010). It had higher filtering accuracy and permeability compared to pure porous aluminum or pure porous titanium materials. However, pore clogging between the matrix and gradient layer is important because of the significant variation in particle size between the Al powder and the Ti-Al mixed powder, which lowers permeability and filtering precision. Ti powder and high purity quartz sheet were used as the raw materials in Liu et al. successful in-situ reaction technique preparation of Ti-Ti $_5$ Si $_3$  gradient composite porous material (Liu et al., 2022).

The findings shown that the maximum pore diameters of the matrix and gradient porous films produced by fine powder sintered at  $1050^{\circ}\text{C}$  under 30~kPa pressure are  $7.8~\mu\text{m}$  and  $6.4~\mu\text{m}$ , and the relative air permeability coefficients of matrix and film are  $56.6~\text{m}^3\cdot\text{m}^{-2}\cdot\text{h}^{-1}\cdot\text{KPa}^{-1}$  and  $9.4~\text{m}^3\cdot\text{m}^{-2}\cdot\text{h}^{-1}\cdot\text{KPa}^{-1}$ . The maximum pore size difference between the porous film and the matrix is negligible, but the relative air permeability coefficient, which is brought on by the reduction in porous film thickness, drops quickly. Researchers have been quite concerned about the Ni-Cr-Mo-Cu multicomponent alloy because of its excellent corrosion resistance and ability to do filtration tasks in highly corrosive settings. In a Ni-Cr-Mo-Cu alloy, the Cr element can create a Cr<sub>2</sub>O<sub>3</sub> oxide coating, according to (Wen et al., 2022). Ni-Cr-Mo-Cu alloy corrosion resistance may be enhanced by this. However, there are not many publications on how well Ni-Cr-Mo-Cu porous materials filter.

In this paper, Ni, Cr, Mo, Cu powder was used as raw material to prepare porous material matrix by activation reaction sintering, and then Ni, Cr, Mo and Cu with larger particle size were painted on the surface of the matrix, and a gradient degree Ni-Cr-Mo-Cu porous material was obtained by vacuum sintering. Ni-Cr-Mo-Cu porous material with first gradient pore size after sintering was used as raw matrix, and Ni-Cr-Mo-Cu porous material with second gradient pore size was obtained by painting the surface with fine particle size Ni, Cr, Mo and Cu. The data of element distribution and pore structure were obtained by characterization.

#### 2. EXPERIMENT

The purity is 99.9%, the particle size is  $38 \sim 74~\mu m$ , and the powder mass ratio is w (Ni): w (Cr): w (Mo): w (Cu) = 55:30:10:5 of each element powder, through the roller ball mill evenly mixed 48 hours after removal, (Zou et al., Cr at 30%, porous Ni-Cr-Mo-Cu material pore structure is the best), and then the mixed powder into the mold, with a pressure of 60MPa pressed to form a  $\Phi25~mm$  raw compact (Xide et al., 2021). By maintaining heat for two hours in a  $1100^{\circ}\text{C}$  vacuum sintering furnace, a porous material matrix made of Ni-Cr-Mo-Cu was produced.

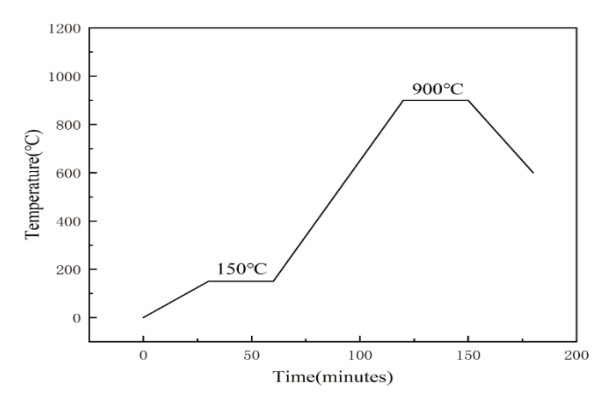


Figure 1: Sintering process

Ni, Cr, Mo, and Cu powders with a purity of 99.9% and a particle size of 20  $\mu m$  were employed as the raw ingredients for the gradient porous film, adopting the same ratio as the matrix. To prepare, 1% stearic acid and alcohol were added to the uniformly mixed powder. It was evenly coated on the surface of the porous support body with a soft brush. After sintering at  $1100^{\circ}\text{C}$  and holding for 2 h, the first-order gradient porous material was obtained and labeled as 1# sample (Jin et al., 2023; Shi et al., 2022; Li et al., 2020; Alcaraz et al., 2023). Then, sample 1# was selected as the original matrix. the element powder mixture with particle size of 7  $\mu m$  was brushed, and the second-order gradient pore size porous material was obtained after vacuum sintering, labeled as sample 2#. The sintering process is shown in Figure 1, 150°C for 30 minutes is to remove impurities such as water vapor, the final sintering temperature is 900°C, 200 degrees lower than the matrix sintering temperature is because of the use of ultrafine-grained powder, the temperature is too high will lead to sample

sintering densification and even make the pores clogged. According to GB 5164-85, the porosity of the porous material samples was measured, and the phase composition and pore structure of the graded Ni-Cr-Mo-Cu porous material were characterized by X-Ray Diffraction (XRD), Scanning Electron Microscope (SEM) and other testing methods.

### 3. RESULTS AND DISCUSSION

#### 3.1 Phase Analysis

Figure 2 shows the XRD patterns of Ni-Cr-Mo-Cu porous material matrix and 1# and 2# samples. As shown in the Figure 1 the phase composition of the matrix after vacuum sintering is Ni, NiCu and Cr1<sub>1.12</sub>Ni<sub>2.88</sub>. The diffraction peaks of 1# and 2# samples do not shift, indicating that their phase composition is the same.

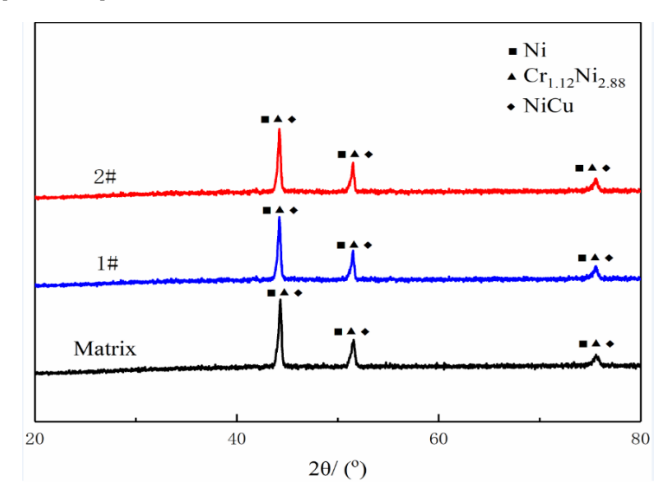


Figure 2: XRD patterns of different samples after vacuum sintering

## 3.2 First Order Gradient Pore Size Ni-Cr-Mo-Cu Porous Material

The SEM surface and side morphology of the first-gradient Ni-Cr-Mo-Cu porous material are shown in Figure 3.

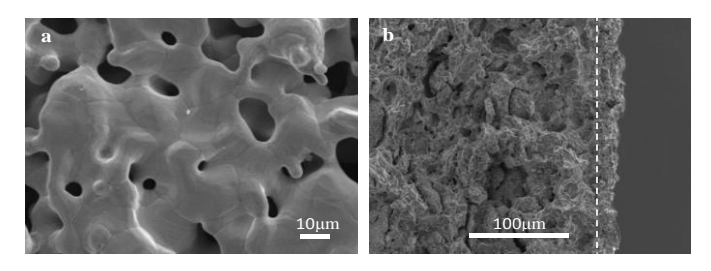


Figure 3: 1# SEM images of sample: (a) Surface; (b) Cross-section

It can be seen from Figure 3 (a) that the film thickness of the 1# sample is uniform and the pores are abundant. The maximum pore size of the material measured by the instrument is  $10.4~\mu m$ , and the permeability is  $83.7~m^3 \cdot m^2 \cdot h^1 \cdot KPa^1$ . This lays a good foundation for the gradient pore size porous materials to have good filtration. It can be seen from Figure 3 (b) that the film layer of sample 1# has a good bond with the support body, and the film thickness is uniform.

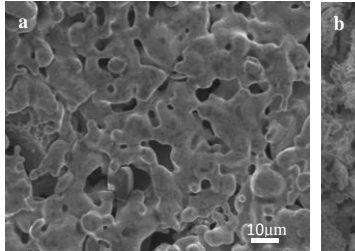
## 3.3 Second Order Gradient Pore Size Ni-Cr-Mo-Cu Porous Materials

In order to systematically study the effect of different particle size differences on gradient porous films, Ni, Cr, Mo, Cu powder with raw material particle size of 20  $\mu m$  and 7  $\mu m$  were used to prepare a gradient porous film and a second gradient porous film, respectively. After testing, the pore structure parameters of the gradient pore size Ni-Cr-Mo-Cu porous material are listed in Table 1.

**Table 1:** Main pore structure parameters of the second order pore- size-gradient porous Ni-Cr-Mo-Cu alloys

8		
Sample	Permeability m³·m⁻²·h⁻¹·KPa⁻¹	Maximum pore size /μm
matrix	96.3	13.3
1#	83.7	10.4
2#	78.9	7.2

It can be seen from Table 1 that compared with the support body, the permeability and maximum pore size of the 1# sample showed a small change. The permeability decreased by 13.1% from  $96.3~m^3 \cdot m^2 \cdot h^{-1} \cdot \text{KPa}^{-1}$  to  $83.7~m^3 \cdot m^2 \cdot h^{-1} \cdot \text{KPa}^{-1}$ , and the maximum pore size decreased by  $10.4~\mu m$ . The permeability of 2# sample decreased by 18.1% compared with the matrix, but the filtration accuracy was greatly improved, and the maximum pore size was maintained at 7.2  $\mu m$ . According to the analysis, the first gradient degree film plays a key role in the preparation of second-order gradient pore size porous materials. Figure 4 shows the SEM plane and side morphology of 2#.



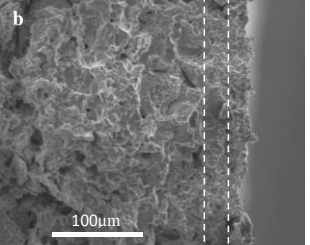
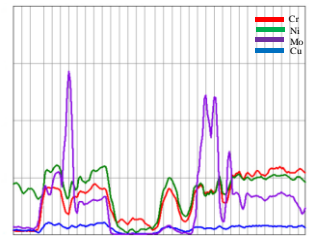
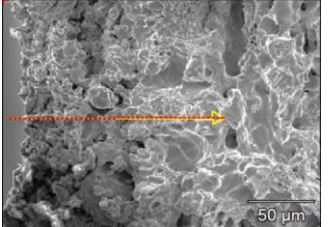


Figure 4: 2# SEM morphology of sample: (a) Surface; (b) Cross-section

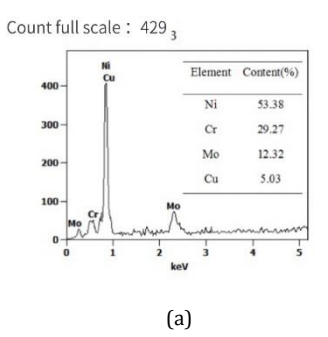
It can be seen from Figure 4 (a) that the pore size is significantly smaller than that of the first-gradient porous material, the distribution between pores is tight, and the pore structure is complete. It can be seen from Figure 4 (b) that the second order gradient pore size porous material consists of a matrix and two membrane layers, and the bond between the membrane layer and the membrane layer is good. It can be seen that the pore size decreases from left to right, indicating that the second-order gradient pore size porous material has a good gradient film structure.

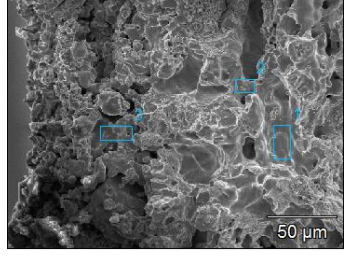
Figure 5 shows the line scanning energy spectrum of porous materials with second-order gradient pore size.



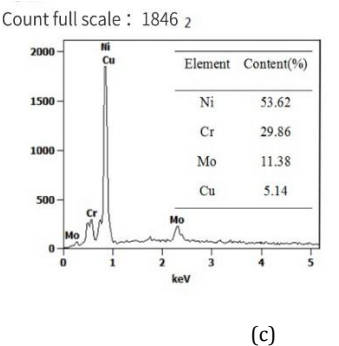


**Figure 5:** (a)2# sample linear scanning spectrum diagram; (b) 2# sample Cross-section





(b)



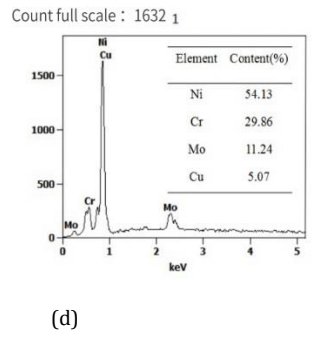


**Figure 6:** (a)2#The cross-section morphology; (b) The Element content diagram at position 1; (c) The Element content diagram at position 2; (d)

The Element content diagram at position 3

From figure 5 (a), it can be seen that the content of Mo element at the boundary increases sharply, which may be caused by the rapid diffusion of Mo element at the boundary, while the content of elements such as Ni Cr Mo Cu in the middle part drops to close to 0 scale, which may be because the element here is a hole and cannot be scanned. It can be seen that the film boundary is clear, the four elements of Ni, Cr, Mo and Cu change alternately, and the changes of the four elements are basically in line with the structure of the film layer, and the content of the four elements is roughly the same as that of the element powder in Figure 5 (b). Figure 6 shows the profile morphology and energy spectrum analysis diagram of the second-order gradient pore size porous material.

Figure 6 (a) shows the cross-section of the sample. Figure 6 (b), (c), and (d) represent the energy spectrum analysis diagrams of positions 1,2, and 3 in the figure respectively. The concentrations of Ni Cr Mo Cu at site 1 were 54.13%, 29.86%, 11.24% and 5.07%, respectively. The concentrations of Ni Cr Mo Cu at site 2 were 53.62%, 29.86%, 11.38% and 5.14%, respectively. The concentrations of Ni Cr Mo Cu at site 3 were 53.38%, 29.27%, 12.32% and 5.03%, respectively. It can be seen from Figure 6 that the pore size of the second order gradient porous material is distributed in a gradient manner, and the results of energy spectrum analysis are roughly the same as the test results of the 1# sample. The difference of powder content in these three places is very small, indicating the uniformity of element distribution.

#### 4. CONCLUSION

Ni-Cr-Mo-Cu porous matrix was prepared from Ni, Cr, Mo and Cu powders by activation reaction sintering method. The porous material with second order gradient pore size was obtained by coating the powders with different sizes. The following conclusions are reached.

A gradient pore size porous material was prepared by brush coating. Ni, Cr, Mo and Cu powder with particle size of 20  $\mu m$  were used as raw materials for gradient porous film layer. The gradient pore size porous material was obtained by vacuum sintering at 1100°C and held for 2 h. The membrane structure is complete, and the maximum pore size is 10.4  $\mu m$ . The permeability is 83.7  $m^3 \cdot m^2 \cdot h^{-1} \cdot KPa^{-1}$ .

Using 20 microns Ni, Cr, Mo, Cu mixed powder modified matrix as a transition layer, 7 microns of Ni, Cr, Mo, Cu mixed powder preparation of the second order gradient pore size as surface film layer Ni, Cr, Mo, Cu porous materials, film has good integrity, zero defect, membrane between layers That can be observed clearly metallurgical combination, With good bonding strength, the filtration accuracy is improved, the maximum pore size is  $7.2 \, \mu m$ , and the permeability is  $78.9 \, m^3 \cdot m^2 \cdot h^{-1} \cdot KPa^{-1}$ .

Due to the excellent filtration performance of second order gradient pore size Ni-Cr-Mo-Cu porous materials, it provides hope for industrial development and practical application, and provides ideas for the filtration direction of metal and ceramic porous materials.

## REFERENCES

Adeniran, J.A., DeKoker, J.J., Akinlabi, E.T., 2017. Sustainable hydrogen generation substrates, catalysts and methods: an overview. 2017 8th International Conference on Mechanical and Intelligent Manufacturing Technologies (ICMIMT). IEEE, Pp. 21-26.

Alcaraz, J.Y.I., Foqué, W., Sharma, A., 2023. Indirect porosity detection and root-cause identification in WAAM. J Intell Manuf.

Ameta, K.L., Solanki, V.S., Singh, V., 2022. Critical appraisal and systematic review of 3D & 4D printing in sustainable and environment-friendly smart manufacturing technologies. Sustainable Materials and Technologies, 34, Pp. e00481.

Hashe, V.T., and Jen, T.C., 2020. Comparative study of Hydrogen yield from magnesium waste products in Acetic acid and Iron chloride solution. 2020 IEEE 11th International Conference on Mechanical and Intelligent Manufacturing Technologies (ICMIMT), Cape town, South Africa, Pp. 182-186.

He, Y.H., Jiang, Y., Xu, N.P., 2010. Fabrication of Ti-Al micro/nanometer-sized porous alloys through the Kirkendall effect. Advanced Materials, 19 (16), Pp. 2102–2106.

Jin, Z., Lim, D.D., Zhao, X., 2023. Machine learning enabled optimization of showerhead design for semiconductor deposition process. J Intell Manuf.

- Lakhdar, Y., Tuck, C., Binner, J., 2021. Additive manufacturing of advanced ceramic materials. Progress in Materials Science, 116, Pp. 100736.
- Li, C., Tang, Y., Cui, L., 2015. A quantitative approach to analyze carbon emissions of CNC-based machining systems. J. Intell Manuf., 26, Pp. 911– 922.
- Li, Y., Feng, Z., Hao, L., 2020. A review on functionally graded materials and structures via additive manufacturing: from multi-scale design to versatile functional properties. Advanced Materials Technologies, 5 (6), Pp. 1900981.
- Li, Y., Jahr, H., Zhou, J., Zadpoor, A.A., 2020. Additively manufactured biodegradable porous metals. Acta Biomater., 115, Pp. 29-50.
- Liu, Z., Gao, B., Liu, Y., Ji, S., Ao, Q., 2022. Research on preparation and characterization of Ti-Ti5Si3 gradient composite porous material via insitu reactive process. Journal of Alloys and Compounds, Pp. 899.
- Shi, S., Si, Y., Han, Y., 2022. Recent progress in protective membranes fabricated via electrospinning: Advanced materials, biomimetic structures, and functional applications. Advanced Materials, 34 (17), Pp. 2107938.
- Uwamungu, J.Y., Kumar, P., Alkhayyat, A., 2022. Future of Water/Wastewater Treatment and Management by Industry 4.0 Integrated Nanocomposite Manufacturing. Journal of Nanomaterials.
- Vaisnav, S.M., Murugesan, S., 2022. Temperature Control Methodology for Catalytic Convertor to Reduce Emissions and Catalyst Aging. In: Reddy, A.N.R., Marla, D. Favorskaya, M.N., Satapathy, S.C. (eds) Intelligent

- Manufacturing and Energy Sustainability. Smart Innovation, Systems and Technologies, vol 265. Springer, Singapore.
- Wang, X., Tuomi, J., Mäkitie, A., 2013. The integrations of biomaterials and rapid prototy techniques for intelligent manufacturing of complex organs. Advances in Biomaterials Science and Applications in Biomedicine; Lazinica, R., Ed, Pp. 437-463.
- Wen, Y., Yang, J., Zhang, C., 2022. High temperature oxidation behavior of porous Ni-Cr-Mo-Cu materials. Chinese Journal of Nonferrous Metals, 32 (8), Pp. 2284-2296.
- Wu, J., Zhang, J., Wang, Z., Qian, G., Zhang, T., 2023. Water-tolerant and antidust CeCo-MnO2 membrane catalysts for low temperature selective catalytic reduction of nitrogen oxides. Journal of Environmental Chemical Engineering, 11(5).
- Xide, L., Yuzuo, L., Bin, L., 2021. Effect of Cr Content on Pore Morphology and Pore-Forming Mechanism of Porous NiCrMoCu Alloys. Rare Metal Materials and Engineering, 50 (5), Pp. 1641-1648.
- Xu, Y., Mustafa, M.Y., Virk, M.S., and Calay, R.K., 2016. Application of numerical analysis in the design and small-scale intelligent manufacturing process of porous fences. 2016 International Symposium on Small-scale Intelligent Manufacturing Systems (SIMS), Narvik, Norway, Pp. 59-63.
- Zhu, J., Wu, P., Chao, Y., 2022. Recent advances in 3D printing for catalytic applications[J]. Chemical Engineering Journal, 433, Pp. 134341.

